PHYSICAL REVIEW D VOLUME 24, NUMBER 7 1 OCTOBER 1981

Primordial sea-quark distribution due to hadronic effects

Sumio Wada
Cavendish Laboratory, University of Cambridge, Cambridge, United Kingdom
(Received 14 October 1980)

The nucleon is a system of an infinite number of quarks and antiquarks due to virtual emission of hadrons. We analyze this phenomenon using a simplified multi-Regge- exchange picture and estimate the primordial sea-quark distribution in the low-Q^2 region.

I. INTRODUCTION

In low-energy phenomenology the nucleon is well described as a system of three valence quarks bound by gluons. This picture is also valid in deep-inelastic scattering in the low-energy region. The momentum carried by the valence quarks is 60% or more for $Q^2 \sim 2$ GeV^2 (Refs. 1 and 2) and the sea-quark distribution is tiny.[1] Even the gluon distribution is relatively minor in the low-Q^2 region. One intriguing approach to the minor sea-quark and gluon distributions is to assume that they vanish at some very small value of Q^2 and to calculate the distribution for larger Q^2 from the evolution equation [or the renormalization-group equation (RGE)].[3,4] This approach has made, at least, a qualitative success and may be regarded as a good zeroth-order approximation.

However, the gluon should exist inside the nucleon to bind valence quarks and we can also argue that the sea quark should exist even in the very-small-Q^2 region due to many-body effects. In fact, the nucleon emits hadrons virtually, which implies that, in patron language, nonvalence antiquarks do exist inside the nucleon. [In the small-Q^2 region, where the quantum-chromodynamics (QCD) coupling constant is not small, we should be careful about ambiguity in the definition of the patron distribution. The present argument may be most clearly understood by having in mind the definition in which a structure function (say, F_2) coincides with the quark and antiquark distribution in all orders.[5]]

The purpose of this paper is to present a semi-qualitative analysis of this phenomenon due to many-body effects. We use the multi-regge-exchange picture of hadron interactions for the analysis. The conclusion is that the magnitude of the calculated sea-quark distribution is small enough and consistent with our phenomenological knowledge from neutrino experiments. Note that we are not proposing an alternative to the QCD approach but are calculating the primordial part of the sea-quark distribution, which is a rather long-distance phenomenon and outside the scope of perturbative QCD. Of course we should confine ourselves to the low-Q^2 region (where the perturbative approach of the RGE is not reliable anyway), and it is the role of the RGE to study how the patron distribution evolves as Q^2 increases for, say, $Q^2 \geq 2$ GeV^2.

This paper is organized as follows. In Sec. II we discuss the multiperipheral picture in patron language and explain how it is related to the primordial sea-quark distribution. We present our formula in Sec. III and analyze it numerically in Sec. IV. Section V is for conclusions.

II. MULTI-REGGE-EXCHANGE MODEL IN THE PARTON PICTURE

The multiperipheral model is a familiar picture to deal with many-particle effects in soft-hadron physics. This model has not only explained various qualitative features of both two-body reactions and many-hadron production, but also a particular version of this picture—the multi-Regge-exchange model with the dual unitarization scheme[6]—has succeeded in giving us a semi-quantitative picture of two-body reactions from the intermediate- to the relatively-high-energy region. The application of the multiperipheral model to deep-inelastic scattering has already been discussed at least in a qualitative level in some references[7,8] and here we extend it to a more quantitative level on the basis of the dual unitarization scheme.

Consider quark diagrams of the multiperipheral process in current-nucleon scattering shown in Fig. 1. The process is understood intuitively in the Breit frame. The initial nucleon emits a hadron, which emits another. The cascade evolves

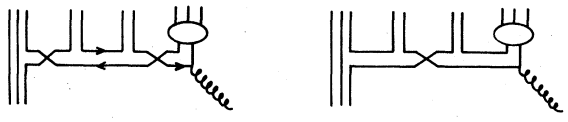

FIG. 1. Quark diagrams of the multiperipheral process in current-nucleon scattering.

and finally a (anti) quark in the last hadron of the cascade chain is hit by the current. Note that only the last stage is a process peculiar to deep-inelastic scattering. We have shown several possible quark diagrams in Fig. 1. If there is a meson exchange with twisted quark lines, the current can hit a (anti) quark which is not a valence quark of the initial nucleon. This is nothing but a sea quark in parton language and is what we analyze in this paper. We do not deal with term (Fig. 2) in which the current directly hits a valence quark, which dominates the structure function in the intermediate and large-x region.

III. FORMALISM

We explain how we calculate the processes shown in Fig. 1 on the basis of the dual-unitarization picture. We will fully use the method and the results in hadron reactions in Ref. 6 to specify our formula and to simplify the calculation.

We start from the diagram shown in Fig. 3(a). Only the final part (the right-most part in Fig. 1) of the Regge exchange is shown explicitly. The rest of the cascade chain is included in the left blob. From the unitarity relation the imaginary part of the amplitude is given as

$$2\,\mathrm{Im}\,T=\sum_{\alpha_1,\alpha_2}\int ds_1 ds_2\rho(s_1)\rho(s_2)\int d\Phi\,|\beta_1|^2\xi_1\xi_2^*\left[\frac{s+Q^2}{(s_1+Q^2)s_2}\right]^{\alpha_1(t)+\alpha_2(t)}|\beta_2|^2, \tag{1}$$

where

$$\xi_i=1\pm e^{i\pi\alpha_i(t)},$$

$$d\Phi=\frac{d^3k_1 d^3k_2}{(2\pi)^6 2E_1 2E_2},$$

and $\rho(s_i)$ is the state density in the s_i part and β_i is the Regge residue. We have used the Regge propagator which takes the mass of the current into account.[8] Only the transversely polarized current is considered here, and so Im $T=2\pi e^2F_1$ (or $2\pi e^2F_3$ for the vector-axial-vector interference).

The left part of Fig. 3(a) is Reggeon-nucleon scattering which also appears in purely hadronic reactions, and it has been shown numerically in Ref. 6 that it can be replaced with the single Reggeon exchange as shown in Fig. 3(b). Therefore, we make the replacement

$$\rho(s_2)|\beta_2|^2\to\sum_\alpha\gamma_\alpha\beta_\alpha s_2^{\alpha(0)}, \tag{2}$$

where $\alpha(0)$, γ_α, and β_α are relevant Regge parameters as indicated in Fig. 3(b).

The right part of Fig. 3(a) is current-Reggeon scattering. We relate this part to the on-shell meson scattering amplitude Im $T_{\alpha_1\alpha_2}$ by the extrapolation using the form of the Veneziano-type amplitude. This extrapolation procedure is known to be successful for various hadronic reactions. The result is

$$\rho(s_1)|\beta_1|^2\langle\xi_1\xi_2^*\rangle_{\mathrm{av}}\to\frac{\alpha'\Gamma^{1/2}(1-\alpha_1(t))\Gamma^{1/2}(1-\alpha_2(t))}{\pi}\mathrm{Im}\,T_{\alpha_1\alpha_2}, \tag{3}$$

where $\langle\ \rangle_{\mathrm{av}}$ indicates the average of an exchange-degenerate pair of Regge trajectories. Note that Im $T_{\alpha_1\alpha_2}$ is only for the valence quarks in the meson so as to avoid the double counting of sea quarks.

Finally we perform the integration of the two-body phase space in Eq. (1) analytically. It becomes possible if we assume Γ in Eq. (3) is a constant. This approximation is legitimate, because the integrand is suppressed exponentially unless t takes a small (negative) value, and because the Γ function is weakly t dependent in this region. In the numerical analysis in Sec. IV we use leading vector and tensor trajectories as α_1 and α_2 in Fig. 3. Therefore, we assume here that $\Gamma=1$ because $1-\alpha_i(t)$ is around one in the dominant region. Using F_1 instead of Im T, Eq. (1) finally becomes

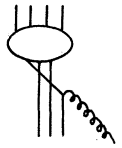

FIG. 2. The quark diagram of direct current-nucleon scattering, i.e., the Born term of the multiperipheral process.

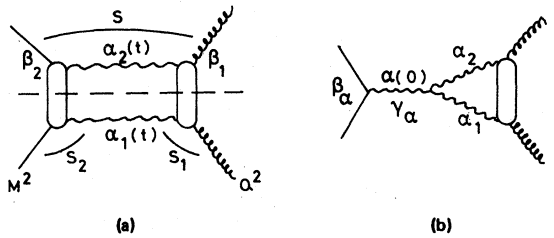

FIG. 3. The unitarity diagram of current-nucleon Regge-exchange scattering (a) and its modification by duality (b).

$$F_1 = \sum_{\alpha,\alpha_1,\alpha_2} \frac{\alpha'\gamma_\alpha\beta_\alpha}{16\pi^2}\lambda^{-1/2}(s,-Q^2,M^2)$$

$$\times \int_{M^2}^{s} ds_1 \int ds_2 F_1^{\alpha_1\alpha_2}\left(\frac{s+Q^2}{s_1+Q^2}\right)^{\alpha_1(0)+\alpha_2(0)} \frac{1}{a} s_2^{\alpha(0)-\alpha_1(0)-\alpha_2(0)}(e^{-2at_{\min}} - e^{-2at_{\max}}), \quad (4)$$

where

$$a = \alpha' \ln\left(\frac{s+Q^2}{(s_1+Q^2)s_2}\right).$$

The energy scale of the Regge propagators above is assumed to be set by α' (=1 GeV^{-2}).[6] The integrand of Eq. (1) shows unphysical behavior in the region $s+Q^2/(s_1+Q^2)s_2<1$ and $t\to-\infty$, which is due to fake behavior of the Regge variable in the low-energy region. This has been discussed in Ref. 6 by studying the dual model. Following their argument we modify the definition of a as

$$a = \alpha' \ln\left[\frac{s+Q^2}{(s_1+Q^2)s_2} + \frac{4}{e}\right]. \quad (5)$$

IV. NUMERICAL ANALYSIS

Here we analyze Eq. (4) [with Eq. (5)] numerically. For the Reggeons α_1 and α_2 (Fig. 3) we take the exchange-degenerate vector-tensor-nonet trajectories of intercepts 0.5, 0.25, and 0. For the Reggeon α we take the Pomeron and the f trajectory. The Regge residue β and the triple-Regge coupling γ are[9,6]

$$\beta_{PNN} = 5.4 \text{ mb}^{1/2}\text{GeV},$$

$$\beta_{fNN} = 6.1 \text{ mb}^{1/2}\text{GeV},$$

$$\gamma = 2.3\,\text{mb}^{-1/2}\text{GeV}^{-3}.$$

γ is assumed to be common for the Pomeron and the f. When the strange Reggeons couple to the Pomeron, γ is reduced by the factor 0.75 or 0.5.[10] For the meson structure function $F_1^{\alpha_1\alpha_2}$ we use the following two forms:

$$\text{A: } F_1^{\alpha_1\alpha_2} \propto 1-x, \qquad \text{B: } F_1^{\alpha_1\alpha_2} = \text{const}. \quad (6)$$

The choice A is consistent with the counting rule and also with the pion structure function recently estimated from the experiments of μ-pair production and high-p_T hadron production.[11] However, there is some experimental indication[12] that the exponent of $1-x$ is smaller in the low-Q^2 region which is our present concern. We will present numerical results for both cases. As the definition of x in case A, we use the Bloom-Gilman variable in the photon-Reggeon system, i.e., $x=Q^2/(s_1+Q^2)$. Note that $F_1^{\alpha_1\alpha_2}$ above is only for the valence quarks of the Reggeons and we should not include Regge behavior ($x^{-1/2}$) to avoid double counting. Regge behavior of the whole structure function automatically appears due to the factor $s_1^{\alpha(0)}$ in Eq. (4). We determine the magnitude of $F_1^{\alpha_1\alpha_2}$ by requiring that two valence quarks carry half of the total momentum of the meson. Because F_1 is linearly related to $F_1^{\alpha_1\alpha_2}$, the following result can be easily converted for other choices of the magnitude.

In Fig. 4 we show the ordinary-antiquark distribution $x\bar{u}$ (=$x\bar{d}$) and the strange-quark distribution xs ($x\bar{s}$) calculated from F_1 [Eqa. (4) and (5)] for case A and case B. The reason for the difference between the two cases becomes relatively easy to see by rewriting Eq. (4) using some new variables, $x_0 \equiv x(1+xM^2/Q^2)^{-1}$ ($\sim x$), $x' \equiv Q^2/(s_1+Q^2)$, and $y \equiv 2\alpha' s_2(s_1+Q^2)/(s-s_1)$:

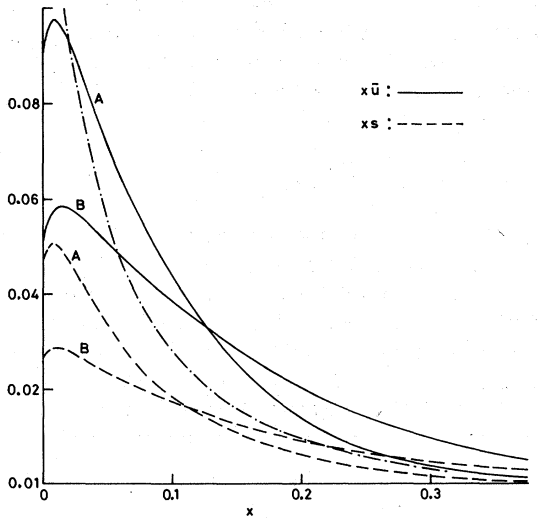

FIG. 4. The distribution of $\bar{u}$ and s at $Q^2=1$ GeV^2 calculated from Eqs. (4) and (5). Here x means the ordinary Bjorken variable. The dashed-dotted line is the result (Ref. 4) of dynamical QCD. See the end of Sec. IV.

$$F_1 = \sum \frac{\alpha'\gamma_\alpha\beta_\alpha}{16\pi^2}\frac{Q^2}{\lambda^{1/2}}2^{-\alpha+\alpha_1+\alpha_2-1}x_0^{-\alpha-1}\int_{x'_{\min}}^{1} dx' F_1^{\alpha_1\alpha_2}(x')x'^{\alpha-1}\left(1-\frac{x_0}{x'}\right)^{\alpha-\alpha_1-\alpha_2+1} \times \frac{1}{a}y^{\alpha-\alpha_1-\alpha_2}(e^{-2at_{\min}}-e^{-2at_{\max}}). \quad (7)$$

The integration region for y is

$$2\alpha' M^2\frac{x_0}{x'-x_0} < y < 2\alpha'(\sqrt{s}-\sqrt{s_1})^2\frac{x_0}{x'-x_0},$$

and $x'_{\min}=Q^2/[(\sqrt{s}-M)^2+Q^2]$ $(\sim x)$. Then we can see that two inequalities,

$$F_{1,A}^{\alpha_1\alpha_2} < F_{1,B}^{\alpha_1\alpha_2} \text{ for large } x,$$

$$\int_0^1 dx' F_{1,A}^{\alpha_1\alpha_2}\, x'^{\alpha-1} > \int_0^1 dx' F_{1,B}^{\alpha_1\alpha_2} x'^{\alpha-1},$$

explain the difference between the two cases in Fig. 4. Regge behavior of $F_1(\propto x^{-\alpha})$ for $x\to 0$ is also obvious from Eq. (7), but due to phase-space effects the behavior $x^{-\alpha}$ is very slow to set in.

We show the second moments of $\bar{u}$ for various Q^2 in Fig. 5. The difference of the second moments between the two cases is very small. In fact, we can prove that for $Q^2\to\infty$ the nth moment of F_1 is proportional to that of $F_1^{\alpha_1\alpha_2}$, which we have assumed to be the same for $n=2$. The shape of $\bar{u}(x)$ is essentially the same as Fig. 4 for all Q^2, and the second moment approaches the value ~ 0.024 as $Q^2\to\infty$. As Q^2 increases F_1 scales simply because we have assumed that $F_1^{\alpha_1\alpha_2}$ does. As was explained in the Introduction, the purpose of the present calculation is to estimate the primordial sea-quark distribution in the low-Q^2 region. As Q^2 increases the RGE gives us a reliable prediction for the Q^2 dependence of the patron distribution. The second moment of $\bar{u}$, in the four-flavor theory, should approach $\frac{3}{56}$ for $Q^2\to\infty$, which is well beyond the values in Fig. 5. Our results should not be taken seriously for, say $Q^2>2$ GeV^2.

The dashed-dotted lines in Figs. 4 and 5 are the sea-quark distribution[4,13] calculated from the RGE (in the leading-logarithm approximation) assuming that only the valence quarks exist inside the nucleon at $Q^2\simeq 0.35$ GeV^2.

V. CONCLUSIONS

In this paper we have analyzed the multi-Regge-exchange process in deep-inelastic scattering so as to estimate the primordial sea-quark distribution in the low-Q^2 region. Our result in Fig. 5 can successfully be compared with the neutrino experiment[1] which suggests that the second moment of the ordinary sea quarks (four times $\bar{u}$) is about 0.06 for $Q^2\simeq 2$ GeV^2. We cannot tell the precise sea-quark distribution for fixed Q^2 experimentally at present. There may be theoretical uncertainties in our formalism itself, and we are not in a position to tell, for example, which choice in Eq. (6) (A or B) is better. However, the authors of Ref. 4, who discussed the parton distribution in the "dynamical" QCD picture (the dashed-dotted lines in Figs. 4 and 5), claimed that their results are consistent with the data except for a possible underestimate of a factor of 2 in the intermediate-x region ($0.2\leq x\leq 0.5$). Comparing their results with ours, we can say that our result is also consistent with the data if it is extrapolated to the higher-Q^2 region by the RGE with an adequate gluon distribution.

As was emphasized before, our aim is to estimate the primordial sea-quark distribution in the low-Q^2 region, and its evolution for higher Q^2 is in the realm of the RGE. So our conclusion here is that we can explain the magnitude of the initial sea-quark distribution theoretically, though not very accurately yet.

Note added. The formalism applied here is based on the conventional multi-Regge picture with some topological arguments, which is purely soft-hadron physics. However, being inspired by the results of two-dimensional QCD [for example, R. C. Brower *et al.*, Nucl. Phys. B128, 175 (1977)], some people tried to apply soft-hadron physics to the hard-parton process and vice versa [see

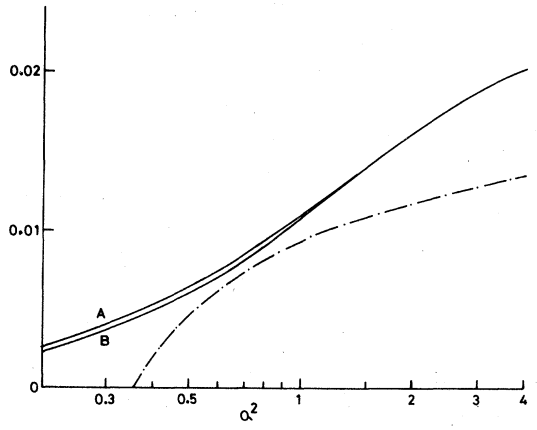

FIG. 5. Q^2 dependence of the second moment of $\bar{u}$. The dashed-dotted line is the result (Ref. 4) of dynamical QCD.

G. Cohen-Tannoudji *et al.*, Phys. Rev. D 19, 3397 (1979) and references therein]. Their basic strategy is to extend topological similarity to dynamical ones. Predicted relations between inclusive cross sections of hadron scattering and fragmentation functions and/or structure functions in deep-inelastic scattering have made some remarkable successes phenomenologically. However, the validity of the dynamical similarity between two processes in the four-dimensional world is not obvious and we need more theoretical consideration about it.

In this paper, we have avoided the discussion on hard-parton dynamics by introducing an empirical meson structure function. By doing so we could calculate the sea-quark distribution in the small-x region. Although the discussion of the sea-quark distribution for $x \to 1$ may become possible by modifying Eq. (1) with the power behavior of large-angle scattering for large t, the valence-quark distribution is beyond the scope of the conventional soft-hadron physics and has nothing to do with the argument in this paper.

ACKNOWLEDGMENTS

The author is indebted to the colleagues of his present and previous institutes for many helpful discussions. He also thanks Paul Rakow for reading the manuscript, and both the Japan Society for Promotion of Science and the United Kingdom Scientific Research Council for financial support.

[1]J. G. H. De Groot *et al.*, Phys. Lett. 82B, 456 (1979); Z. Phys. 1, 143 (1979).
[2]L. F. Abbott, W. B. Atwood, and R. M. Barrett, Phys. Rev. D 22, 582 (1980); S. P. Luttrell and S. Wada, Nucl. Phys. B182, 381 (1981).
[3]G. Parisi and R. Petronzio, Phys. Lett. 62B, 331 (1976); V. A. Novikov *et al.*, Ann. Phys. (N.Y.) 105, 276 (1977).
[4]M. Glück and E. Reya, Nucl. Phys. B130, 76 (1977); E. Reya, Phys. Rep. 69, 195 (1981).
[5]G. Altarelli, R. K. Ellis, and G. Martinelli, Nucl. Phys. B143, 521 (1978).
[6]H. M. Chan, J. E. Paton, and S. T. Tsou, Nucl. Phys. B86, 479 (1976).
[7]M. J. Creutz, Phys. Rev. 187, 2093 (1969); S. S. Shei and D. M. Tow, Phys. Rev. D 4, 2056 (1971).
[8]C. J. Hamer, Phys. Rev. D 10, 1458 (1974).
[9]V. Barger and R. J. N. Phillips, Nucl. Phys. B32, 93 (1971).
[10]R. Carlitz, M. B. Green, and A. Zee, Phys. Rev. D 4, 3439 (1971).
[11]C. B. Newman *et al.*, Phys. Rev. Lett. 42, 951 (1979); M. D. Corcoran *et al.*, *ibid.* 44, 514 (1980); K.-W. Lai and R. L. Thews, *ibid.* 44, 1729 (1980).
[12]D. McCal *et al.*, Phys. Lett. 85B, 432 (1979).
[13]J. F. Owens and E. Reya, Phys. Rev. D 17, 3003 (1978).